



Comparative Analysis About Degradation Mechanisms of Printed Circuit Boards (PCBs) in Slow and Fast Pyrolysis: The Influence of Heating Speed

Fabian Diaz¹ · Benedikt Flerus^{1,2} · Samant Nagraj¹ · Katrin Bokelmann² · Rudolf Stauber² · Bernd Friedrich¹

Published online: 15 February 2018
© The Minerals, Metals & Materials Society 2018

Abstract

Despite the high number of publications regarding pyrolysis of electronic scraps, there have not been many attempts to correctly understand the degradation mechanisms of organics. Hence, it is a challenge to identify the optimum parameters that can benefit its metallurgical recycling and especially the recovery of technological elements. This article refers to a detailed analysis of the degradation mechanisms during slow pyrolysis as well as its deflection under fast heating speed. The analysis was made based on continuous off-gas analysis by Fourier transform infrared spectroscopy (FTIR), kinetic analysis on slow pyrolysis and measurement of total carbon (TC), total organic carbon (TOC), and elemental carbon (EC) in solid products at different pyrolysis temperatures. Results have evidenced that degradation of organics in pyrolysis of PCBs takes place in at least three different stages, which are driven by different reaction mechanisms and kinetic conditions. In addition, fast pyrolysis has shown to be beneficial if operated above 600 °C, where high-quality syngas is produced, containing elevated concentrations of CH₄ and H₂, and a lower concentration of H₂O_(g) compared to conventional pyrolysis and fast pyrolysis at lower temperatures.

Keywords WEEE · Pyrolysis · Recycling · Printed circuit boards · Thermal pre-processing

Introduction

With the developing trend in technology, the demand for electric and electronic equipment around the world is increasing every day. In 2014 alone, 41.8 million tons (5.7 kilograms per inhabitant (kg/inh.)) of waste electric and electronic equipment have been generated worldwide and this number is estimated to rise up to 50 million tons by 2018 (6.7 kg/inh.) [1].

Many environmental protection agencies around the world consider waste electric and electronic equipment

(WEEE) to be hazardous because of the presence of inorganic compounds such as nickel, antimony, arsenic mercury, lead, cadmium, and chromium and organic compounds such as chlorofluorocarbons, polychlorinated biphenyls, polyhalogenated, and polycyclic aromatic hydrocarbons [2]. Therefore, it is necessary to study efficient alternatives for its recycling, which allows proper control of the harmful elements and allow proper recovery of valuable metals.

Recycling of WEEE is also an important subject in terms of potentially recovering valuable elements such as gold, silver, etc. Indeed, the major economic driver for recycling WEEE is the recovery of precious metals due to their high economic value. Precious metals are widely used in electronics due to their high chemical stability and electric conductivity, making them a valuable contact material. Therefore, these elements make up more than 70% of the value of cell phones, calculators, and printed circuit board scraps [3].

Printed circuit boards (PCBs) are a significant part of almost all EEE. They are a platform upon which micro-electronic components like capacitors, transistors, and

The contributing editor for this article was Sharif Jahanshahi.

✉ Fabian Diaz
fdiaz@ime-aachen.de

¹ Institute of Process Metallurgy and Metal Recycling IME, RWTH Aachen University, Intzestraße 3, 52056 Aachen, Germany

² Fraunhofer Institute for Silicate Research ISC, Project Group Materials Recycling and Resource Strategies IWKS, Brentanostraße 2, 63755 Alzenau, Germany

microchips are mounted. They are a complex mixture composed of around 40% metals, 30% polymers, and 30% ceramics. However, there is a great variance in composition of PCB wastes from different appliances, manufacturers, and of different age.

Table 1 shows some typical waste PCB material composition [4–7]. Waste PCBs account for around 3% by weight of the mass of global WEEE. However, the recycling of waste printed circuit boards (WPCBs) has been a challenge due to its heterogeneous composition. The main value in PCBs is their content in copper and precious metals, usually recovered by traditional metallurgical processes such as pyro-metallurgy, hydro-metallurgy, and more recently by biotechnology processes [8].

The fact that WEEE scraps correspond to a very heterogeneous group of materials in terms of concentrations of organics, halogens, and metals leads to some limiting factors regarding metallurgical processing. The main ones can be listed as follows: overheating of the furnace due to uncontrollable combustion, capacity and life time of the off-gas system due to increased amount of volatile matter, high risk of corrosion of refractory materials in the furnace due to the presence of halogens (e.g., Cl

and Br) and difficulties in the process control due to inhomogeneous chemical composition, which makes a proper slag design very difficult. This effect can be remarkable for materials that contain low metal concentration, which makes the material not attractive enough for the metallurgical industry, generating the so called “rest fractions” that are either incinerated or sent to public landfills. Therefore, pyrolysis as a promising technology for pre-processing of WEEE scraps has been studied.

Theory of Pyrolysis Processing

Pyrolysis is a thermochemical process, where organic material decomposes at elevated temperatures in the absence of oxygen, using a vacuum or inert atmosphere to produce oil, gas, and char [4].

Pyrolysis converts organics by thermal decomposition over a broad temperatures range (300–900 °C) in atmospheres with total absence or small amount of oxygen, in which the structure of polymers breaks down into smaller intermediate products at different temperatures, also called cracking [4, 9]. The products produced after thermal

Table 1 Material composition of different waste PCBs

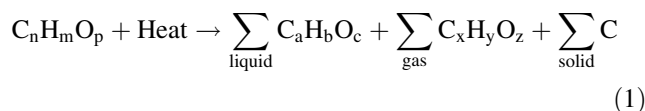
Materials	Wt.% [4]	Wt.% [5]	Wt.% [6]	Wt.% [7]
Metals				
Copper (Cu)	20	15.6	22	26.8
Aluminum (Al)	2	–	–	4.7
Lead (Pb)	2	1.35	1.55	–
Zinc (Zn)	1	0.16	–	1.5
Nickel (Ni)	2	0.28	0.32	0.47
Iron (Fe)	8	1.4	3.6	5.3
Tin (Sn)	4	3.24	2.6	1
Antimony (Sb)	0.4	–	–	0.06
Gold (Au)/ppm	1000	420	350	80
Silver (Ag)/ppm	2000	1240	–	3300
Palladium (Pd)	50	10	–	–
Ceramics				
SiO ₂	15	41.86	30	15
Al ₂ O ₃	6	6.97	–	–
Alkaline and alkaline earth oxides	6	CaO 9.95 MgO 0.48	–	–
Titanates, mica	3	–	–	–
Plastics				
Polyethylene (PE)	9.9	–	16	–
Polypropylene (PP)	4.8	–	–	–
Polyesters (PS)	4.8	–	–	–
Epoxies	4.8	–	–	–
Polytetra-fluoroethane (PTFE)	2.4	–	–	–
Polyvinyl-chloride (PVC)	2.4	–	–	–
Nylon	0.9	–	–	–

degradation of polymers are volatile at elevated temperatures and go to the gas or oil fractions, whereas metals and inorganic materials (glass fiber) generally remain unchanged and accumulate in the residue. Figure 1 explains the degradation mechanism of organics with temperature [10].

Pyrolysis appears to be an emerging option in WEEE recycling technology, facilitating the recovery of high value, potentially accessible products such as precious metals, fuel, and chemicals [13]. During the pyrolysis of WPCBs, it is not only possible to break the organic part in order to obtain fuel or useful chemicals, but further processing of the solid product can enable the recovery of valuable metals more easily and efficiently [14].

During cracking of hydrocarbons, many reactions take place and most of them are based on free radicals, which are atoms, molecules, or ions, which possess unpaired valance electrons. Radicals are formed when covalent bonds in the molecule break, which usually happens at elevated temperatures, when enough energy is available to break the bond. These free radicals are highly reactive towards other substances [15].

During pyrolysis, the principal objective is to break down the long-chain molecules (polymers) into simple or short-chain molecules (monomers or oligomers) in an inert atmosphere or vacuum, yielding three types of products: condensable volatile matter, non-condensable volatile matter, and a carbon-rich solid residue named as pyrolysis char. Equation (1) illustrates the different reactions taking place during pyrolysis [16].

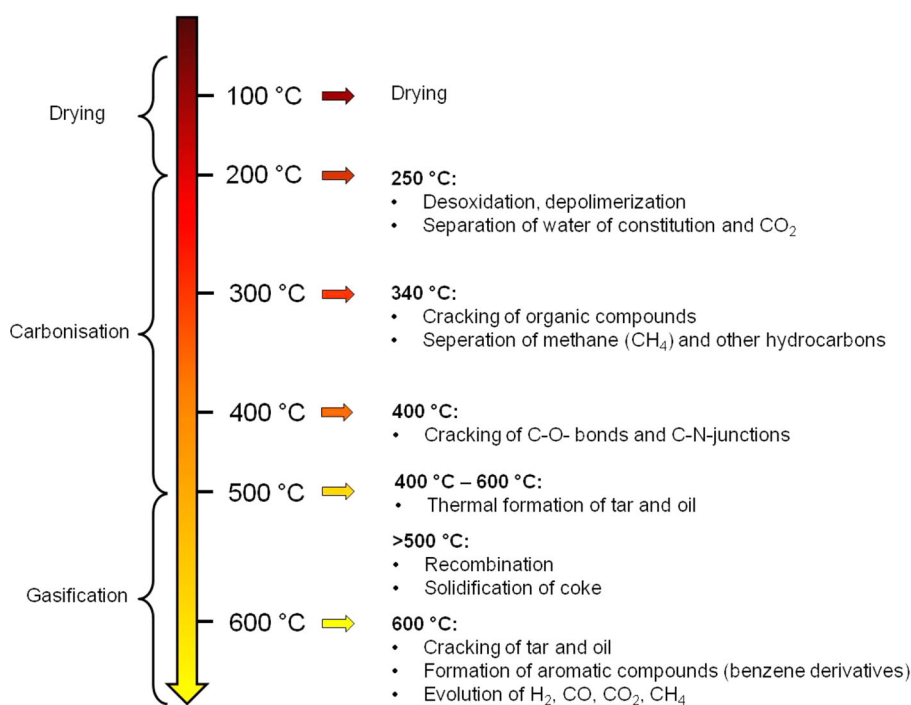


The pyrolysis tar obtained during the pyrolysis process is a mixture of organic compounds, containing some aqueous products appearing as a thick, black, highly viscous liquid composed of complex mixture of condensable hydrocarbons, including oxygen containing 1–5 ring aromatic and complex polyaromatic hydrocarbons [17, 18].

Tar is produced primarily by de-polymerization during the pyrolysis stage of gasification. The formation of primary tar begins at relatively low temperatures (200 °C) and is completed at 500 °C by breaking down of complex and long-chain organic compounds. Char is also produced during this stage. Above 500 °C, the primary tar components (alcohols, ketones, aldehydes, phenols, furans, and mixed oxygenates [19]) start reforming into smaller, lighter non-condensable gases and a series of heavier molecules called secondary tar (phenols and olefins are primary constituents). H₂O vapor is produced as well as non-condensable gases that include CO₂ and CO. At still higher temperatures, primary tar products are destroyed and tertiary products are produced (methyl acenaphthylene, methylnaphthalene, toluene, and indene [20]).

Furthermore, other products from pyrolysis are the pyrolysis gases, which mainly consist of hydrogen, carbon dioxide, carbon monoxide, oxygen, methane with all the C1–C4 alkanes and alkenes present in addition to inorganic halogens. The increase of the temperature leads to

Fig. 1 Degradation mechanism of organics during pyrolysis based on [10–12]. (Color figure online)



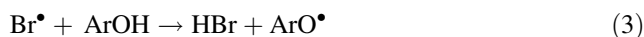
significant amounts of CH₄ and H₂, while the amount of C₂–C₄ hydrocarbons will decrease [21].

At the end of the pyrolysis process of PCBs a solid char is produced, which mainly consists of glass fibers, metals, and carbon. The production of carbon in thermoplastic pyrolysis is usually quite low and results from secondary tar-cracking reactions involving the polymerization of unsaturated products such as dienes and olefins or coke precursors, such as aromatics. Therefore, in some cases, this solid fraction is also known as coke [8, 22].

Previous work, reported at IME Process Metallurgy and Metal Recycling Institute, demonstrated that pyrolysis is a viable method to remove halogens from WEEE scraps containing organics. For the particular case of PCBs, it was reported that bromine and chlorine can be removed with up to 77 and 79% effectiveness, respectively [23]. However, it is evidenced that halogens leave the system with the pyrolysis gases. The pyrolysis process has a major disadvantage in generating toxic HBr as one of the main gaseous species. Attention must be given to control the chemically toxic gases in the pyrolysis process. With ever increasing restrictions on the amounts of toxic gases released to the atmosphere, the viability of pyrolysis as a recycling method for waste PCBs will depend on the ability of this process to control the toxic gases (especially HBr) released during processing [8, 24].

There are already several studies discussing the off-gas formation during the pyrolytic degradation of PCBs. Jie et al. have investigated the formation of H₂, CH₄, CO, and CO₂ at different temperatures but low heating speed. It was concluded that there is no further temperature influence on gaseous products above 500 °C where the pyrolysis gas is rich in H₂ and CH₄ [25]. Detailed work in terms of HBr and formation of brominated compounds during pyrolysis was done by Barontini and Cozzani, as well as Chien et al. Both concluded that high temperatures and fast heating promote the formation of HBr [26, 27]. The mechanism for HBr generation can be specified by the decomposition of brominated bisphenol A and the simultaneous formation of bromine radicals, which are able to separate hydrogen from

other hydrocarbon molecules (RH and phenols (ArOH)) to form HBr [26]:



where Ar stands for Aromatic ring attached to an OH group or free oxygen radical, RH for organic compounds and R[•] for free organic radical.

Pyrolysis Operating Conditions

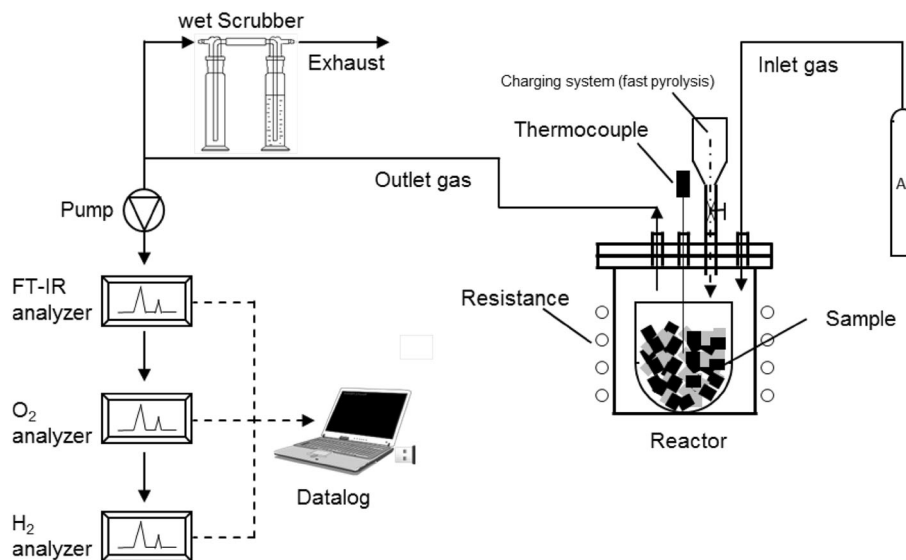
The composition of pyrolysis products can be strongly affected by the process condition. Table 2 shows the most relevant operating conditions during pyrolysis of plastic based products. The modification of these parameters will in turn modify the product distribution resulting from the thermal decomposition process, whereby the chemical composition is mainly influenced by two fundamentals. On the one hand, mass conservation states that pyrolysis products in the three phases (gas, liquid, and solid) are made up from the same constituents as the raw material. Therefore, their relative amounts are conserved. In other words, pertinent elements redistribute during the pyrolysis, such as chlorine and hydrogen enriched in the gas phase whereas carbon will be gathered in the coke. On the other hand, a straight link between polymer structure and its primary pyrolysis product exists. This means that the products are always formed after a bond breakage of the initial material, accompanied by a molecular or free radical rearrangement, in which increasing temperatures promote the bond breakage [28].

Temperature is perhaps the most relevant parameter since it will directly influence the rate of thermal decomposition and the stability of input material and reaction products. A distinction can be made according to the temperature at which the pyrolysis advances: low (< 400 °C), medium (400–600 °C), or high (> 600 °C). Temperatures above 600 °C combined with vacuum, allow the formation of simple small gaseous bubbles. In contrast, temperatures above 400 °C and increased pressure result in

Table 2 Main pyrolysis parameters and their effects [28]

Parameter	Effect
Chemical composition of the polymer	Primary pyrolysis products are directly related to chemical composition and structure of feedstock and to the mechanism of decomposition
Temperature and heating rate	Higher temperatures and higher heating rates intensify the bond breaking and the production of small molecules
Residence time	Longer residence time reduces primary products, yielding more stable products like coke, char, and methane
Reactor type	It determines the quality of heat transfer, mixing, and residence time of gaseous and liquid phases
Operating pressure	Low pressures will decrease the formation of reactive fragments forming cokes
Presence of reactive gases	Presence of external gases generate heat, dilutes products and directly affect equilibrium, kinetics and mechanisms

Fig. 2 Experimental setup for slow and fast pyrolysis of printed circuit boards (PCBs)



more viscous liquid products, higher rates of pyrolysis, a higher coking tendency, increased amount of secondary products and more dehydrogenation. The pyrolysis of most plastics starts at approximately 300 °C; however, this onset temperature is strongly affected by the presence of additives, flame retardants, stabilizers etc. in the plastic [28].

The residence time is intimately related to the reaction temperature. Short residence times will end up in the formation of monomers (primary products). If more thermodynamically stable products (molecular hydrogen, methane, carbon) are desired, the residence time should be increased [28].

Innovative Approach and Importance of Pyrolysis in Recycling of WEEE

In all studies existing so far, neither the time-dependent evolution of gas components, nor the interaction between the evolved gases during the pyrolysis of printed circuit is discussed. Therefore, two different approaches concerning the analysis of gaseous products are examined in this study. As a first step, the material is heated up slowly, which effects a fractional evolution of different gas products, revealing the preferred evolution temperature of each compound and different stages of thermal decomposition. However, due to the ramped temperature, this slow pyrolysis is both temperature and time dependent, which means that the behavior of compounds already released at 400 °C could not be studied at 700 °C as well as interactions between gases that are released at different temperatures. Hence, the issue of temperature dependency is solved by feeding material into the hot reactor at predefined temperatures, effecting a rapid heating of the material. Thus, the central question refers to the influence

of the heating rate on pyrolysis products, specifically off-gas composition and carbon content in the solid residue of pyrolysed PCBs. In the end, the two methods—slow and fast pyrolysis—are compared in order to verify their validity as a procedure to investigate the mechanisms during the pyrolysis of PCBs. Additionally, a new approach compared to recent literature is the continuous off-gas analysis by Fourier transform infrared spectroscopy (FTIR), so that a real-time record is obtained for all experiments.

Experimental

The pyrolysis tests are done in a programmable resistance furnace. For this purpose, a pyrolysis reactor was manufactured and placed inside the furnace as indicated in Fig. 2. The reactor has a volume of 1 L and is sealed with a lid to create a fully closed system. The top portion of the reactor is water cooled to avoid thermal degradation of the rubber gasket used to seal the reactor. The reactor top contains a pressure gauge, a gas sampling vent, a thermocouple, a carrier gas inlet and an exhaust. In addition to the furnace, a pump manufactured by ASYCO and a FTIR (Fourier transform infrared) gas analyzer made by Gasetm is necessary to conduct the experiments. The pump is in charge of pumping the gas product from the pyrolysis reactor directly into the gas analyzer. Since the gas should reach the gas analyzer without any condensation, the hose is internally heated to a temperature of 180 °C. The gas analyzer has a corrosion-resistant sample cell that is also heated to 180 °C, which ensures that the sample stays in gaseous phase even with high concentrations of water or corrosive gases. The gas analyzer Gasetm DX4000 is

equipped with a software (Calcmeter) which displays the concentration results in ppm, mg/Nm or vol%. Using this equipment, gaseous components, like H₂O, CO₂, CO, NO, NO₂, N₂O, SO₂, NH₃, CH₄, HCl, HF, and other volatile organic compounds (VOCs) such as aliphatics and aromatics can be measured. The reactor top is connected with the gas inlet (argon) and the exhaust, which ends up in the scrubber. The latter consists of two bottles, whereby the second bottle contains distilled water to clean the off-gas and to prevent oxygen back flow into the reactor, whereas the first bottle acts as a safety to prevent water ingress from the second bottle into the reactor in case of a pressure drop inside the reactor. The FTIR pump is adjusted to 2 L/min, whereas the O₂ analyzer pump is adjusted to 30 L/h.

Setup for Slow Pyrolysis

The slow pyrolysis is characterized by a slow heating rate (10 °C/min). For this test, an aluminum oxide crucible is charged with 10 g of pre-shredded PCBs with particle size up to 2 cm and placed inside the reactor. The thermocouple is adjusted to the center of the crucible to monitor the actual temperature during the process. During the experiments, the heating rate of the furnace is maintained at 600 °C/h with a dwell time of 1 h. Afterwards, the furnace is shut off and cooled down. During the process, argon is injected at 6 L/min throughout the experiment in order to avoid any entrance of oxygen.

In this work, the kinetics of the reactions (reaction rate, reaction rate constant, order of the reaction, activation energy, and Arrhenius coefficient) during pyrolysis and combustion of PCBs is also investigated using simultaneous thermogravimetric and differential thermal analysis. The experiments are performed in a Netzsch thermobalance STA 409 by first placing the sample of 100 mg in an alumina (Al₂O₃) crucible inside the analyzer. The process temperature is 1400 °C at 10 °C/min, whereby argon, air, and oxygen are used to maintain defined gas atmospheres. The flow rate of the carrier gas is kept at 1 mL/min. The sample of 100 mg used for the kinetic analysis corresponds to the non-metallic PCB fraction, which can be considered representative as the material is constant for all the trials in this study. It is also important to mention that the material (~ 1 kg) was cryogenically milled and sieved in such a way that the non-metallic fraction reached a particle size smaller than 125 µm of homogenous characteristics and all metals were pulled out. This approach cannot be applied for analysis of metals, which composition varies drastically from one sample to other. It is worth noting that this study focuses only in the degradation mechanism of organics from PCBs and no considerations about metals nor oxides are going to be discussed in this article.

Setup for Fast Pyrolysis

For the fast pyrolysis experiments, shredded printed circuit boards are used as input material. Prior to the pyrolysis experiments, the PCBs are treated in a cutting mill to obtain a maximum grain size of 4 mm, which is required to fill the material into the hot reactor easily. Several samples of 6.5 g are taken from 1.8 kg of shredded PCBs by a rotary cone sample divider to reach a homogeneous composition of every sample.

In total, five fast pyrolysis experiments are performed at 300, 400, 500, 600, and 700 °C. In every experiment, the reactor is purged with 4 L/min of argon. Different to the slow-pyrolysis-experiments, a hole in the cover plate of the reactor is designated as the charging hole for the shredded PCBs. During heating the reactor, the charging hole is closed with a steel plug. At the moment of charging, the plug is replaced by an alumina tube with an affixed funnel at the top end, so that one sample of shredded PCBs can be filled into the reactor, falling through the tube into an alumina crucible at the bottom of the reactor. Afterwards, the alumina tube and the plug are swapped again. While pyrolysis takes place, the off-gas composition is recorded via FTIR.

The solid residue from the fast pyrolysis is processed in a ball mill to separate metallic particles from the non-metallic fraction. The carbon analysis of the non-metallic fraction, having a grain size of < 90 µm, is realized by a LECO R612 multiphase carbon determinator. In particular, total organic (TOC), total inorganic (TIC), elemental (EC), and total carbon (TC) are measured.

Results and Discussion

The chemical composition of this particular material before and after the pyrolysis process has been already discussed in a previous publication. Nevertheless, a table with the chemical composition before and after pyrolysis is shown in Table 3. Further details about dehalogenation effect as well as metal/oxides concentrations can be found in the Reference [23].

Pyrolysis of WEEE Under Slow Heating Rate

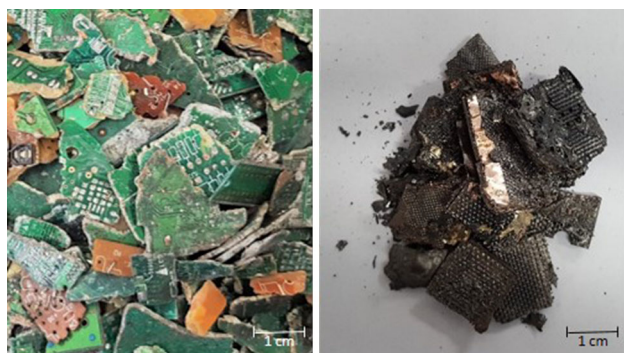
For the slow pyrolysis of PCBs, the maximum temperature is 832 °C. After the process, 32.8% of the material is converted into volatile matter and the solid product corresponds to a brittle material composed mainly of carbon, glass fibers, and copper foils. The material before and after pyrolysis is shown in Fig. 3.

As can be seen in the FTIR records depicted in Fig. 4, the process starts with a dehydration process with some traces of water vapor above 100 °C. Notice that, the

Table 3 Chemical composition of the investigated PCBs and solid product after pyrolysis

Units	Element	Input material	Solid product (700 °C)
ppm	Ag	226	567
	Au	6.52	10.25
wt. %	Cu	15.26	26.38
	Zn	0.12	0.28
	Sn	1.73	2.88
	Pb	0.77	1.25
	Ni	0.02	0.06
	Sb	0.22	0.39
	Al	1.61	3.1
	Si	5.3	10.43
	Ca	3.87	7.32
	Fe	0.1	0.19
	Cl	0.12	0.03
	Br	9.62	2.19
	C	31.65	18.97
	O	24.66	16.57
	H	3.54	0.49
	N	0.64	0.5
kJ/kg	Cp	13687.6	8054.9

moisture content is about 0.6% in the PCBs. After that, at least three cracking periods of the organic material can be distinguished. The first cracking period (220–345 °C) is very short and intense. Between 309 and 336 °C, white smoke can be observed in the scrubber. During this period, a breakdown of long-chain molecules into short-chain hydrocarbons takes place, producing gaseous compounds such as CO₂, CO, H₂O, H₂, and oils such as phenol and tar, and free carbon. The second cracking period occurs from 345 to 575 °C, when the cracking of aliphatic bonds and evolution of methane gas are evident. During this period, no formation of CO or CO₂ can be detected (see Figs. 4 and 5), which indicates that neither oxidation, nor reverse methanation reaction take place. However, a

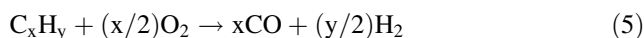
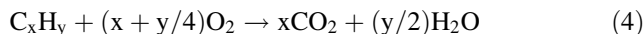
**Fig. 3** Appearance of PCBs before pyrolysis (left) and after pyrolysis (right). (Color figure online)

stable formation of hydrocarbons is shown in Fig. 4. Finally, during the third long cracking period (from 577 °C), tar starts to crack to form methane, phenol, and carbon monoxide. The phenol is again cracked into carbon monoxide, hydrogen, and free carbon.

During the first cracking period, up to 4100 ppm of CO₂ is produced, but the amount of CO produced from the entire process is higher. There is no free oxygen produced during the process. Related to the initial mass of PCB, approximately 70.6 mL/g of H₂O, 50.4 mL/g of H₂, 12.3 mL/g of CO, 5.4 mL/g of CO₂, 16 mL/g of halogens, and 32 mL/g of hydrocarbons are generated from cracking of polymers during the process.

Gases like CO₂, CO, and H₂O formed during pyrolysis are mainly products from combustion reactions like indicated in Eqs. (4) and (5). However, it is very unlikely that pure oxygen would be formed during the process. This assumption is based on several number of experiments on pyrolysis under different parameters and no records of oxygen being measured. Therefore, oxidation of hydrocarbons is more likely due to reactions of those with strong oxidants like hydroxyl radicals. As indicated in Fig. 5, the presence of hydroxyl radicals can easily result from the presence of hydroxyl containing radicals like cresols (p- and m-group) from the aromatic groups and acetic acid (CH₃COOH).

Combustion of hydrocarbons: [16, 29]



As shown in Fig. 5, ethane is shortly present in the off-gas. This molecule experiences cracking reactions that could also be evidenced in the off-gas composition. The strongest formation of ethane is noted at around 300 °C and its concentrations decrease drastically while other short molecules are increasing. Equations (6)–(10) show the mechanism of ethane cracking. When a covalent bond in the ethane molecule is broken, two methyl radicals are formed. This methyl radical strips the hydrogen from another ethyl molecule to become stable. Now, the unstable ethyl radical will break into two molecules of methylene and a hydrogen radical or it can combine with other free radicals to form a single and long free radical, which is mostly unlikely [30, 31]. The previous can be noted during pyrolysis, as formation of methane and hydrogen identified at 300 °C and seem stable during the whole process which ended at around 800 °C.



Fig. 4 Off-gas composition during pyrolysis of PCBs with max. temperature of 832 °C under argon atmosphere

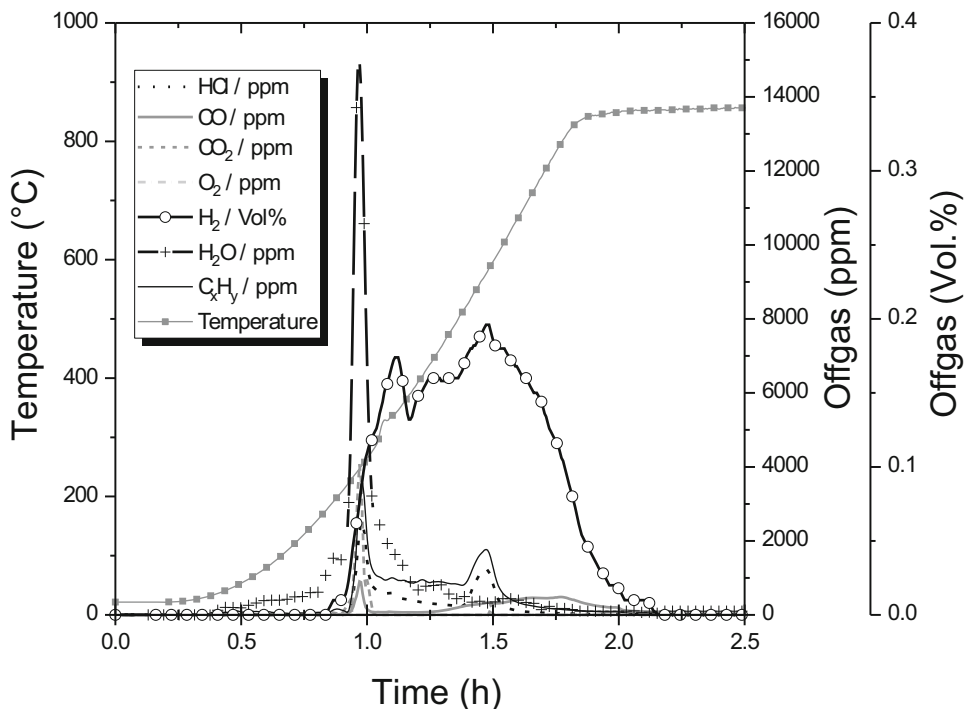
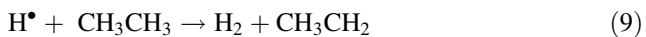
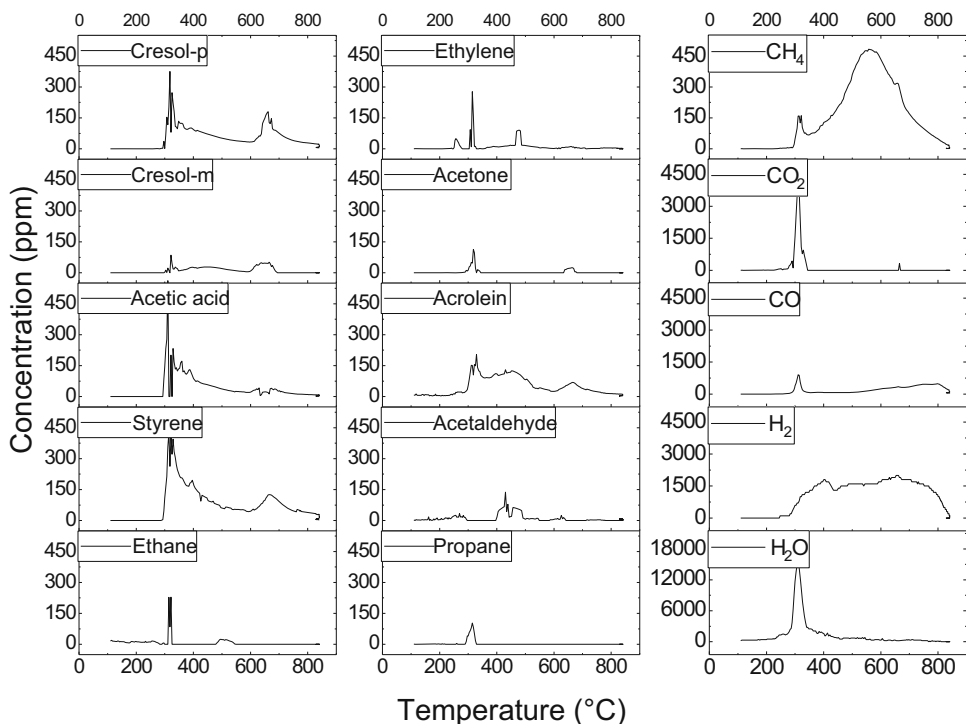


Fig. 5 Comparison between main off-gas products from pyrolysis of PCBs vs. temperature



In order to understand the kinetics of the process, differential thermal analysis (DTA) and thermogravimetric analysis (TGA) of pyrolysis were carried out. In Fig. 6, the DTA (dashed lines) and TGA (solid lines) of PCBs in argon, air, and oxygen atmospheres are shown. Despite the fact that pyrolysis is the main focus in this article, data for

the combustion with air and oxygen are presented to provide a reference to the pyrolysis process.

From the solid lines in Fig. 6, it can be seen that there is an initial stage of degradation in all atmospheres at around 100 °C which corresponds to the dehydration process as already evidenced in the off-gas (see Fig. 4) with the presence of water vapor.

During combustion of PCBs with air or pure oxygen, three stages of degradation are observed, each happening at different rates and at different temperatures. Table 4 gives information about the three stages of degradation and their respective temperature ranges. The first stage of degradation is combustion with oxygen (271 °C) followed by combustion with air (275 °C) and pyrolysis (285 °C), respectively.

After comparing FTIR and TGA/DTA results, it is possible to deduce that during combustion, over 98% of the material degrades during the first two stages, because most of the hydrogen and carbon in the material react below 500 °C with oxygen and below 800 °C with air. During pyrolysis, the long-chain-hydrocarbons are cracked to form tar and other gaseous compounds. In the second stage, the tar formed in first stage is further decomposed to form carbon with still some tertiary tar. In the third stage, this tertiary tar is finally broken down into carbon (coke). In the case of combustion, the production of tar is minimized due to gasification of carbon, which increases the gasification rate with increased amount of oxygen in the carrier gas, which is evidenced by the degradation rate. As indicated in Table 4, the increased amount of oxygen strongly increases the degradation rate in stage I being up to 54% faster compared to pyrolysis.

From the DTA curves, it can be noted that an abrupt exothermic reaction takes place at approx. 300 °C when combustion using pure oxygen occurs. During this period, the maximum amount of material is oxidized, whereas in the case of air, the rate of oxidation decreases and the amount of energy released is also decreased.

Different to combustion, the heat released at pyrolytic conditions is significantly lower, compared to any combustion tests. This might be due to the fact that the energy released during combustion of molecules and the energy supplied is also utilized to break other molecules. In addition, the amount of heat released during pyrolysis varies from time to time, which indicates that de-polymerization involves very complex reactions, which occur in more than one step. However, at least two main exothermic reactions occur at the first (285–405 °C) and third (> 600 °C) cracking period.

One of the main advantages of the TGA is the possibility to determine the kinetic parameters of the reactions during the process. Using the data obtained from the analysis, the calculation of kinetic parameters is possible by means of the equations based on the classical kinetic theory [32]. Calculation of kinetic parameters from the TGA data is based on the following equation:

$$\frac{dW}{dt} = kW^n, \quad (11)$$

where W is the weight of sample undergoing reaction (mg); n is the order of reaction; k is the specific rate constant (1/min), and t is the time (min). The rate constant k changes with absolute temperature according to the following Arrhenius equation:

Fig. 6 DTA and TGA of PCBs during pyrolysis and combustion (air and oxygen)

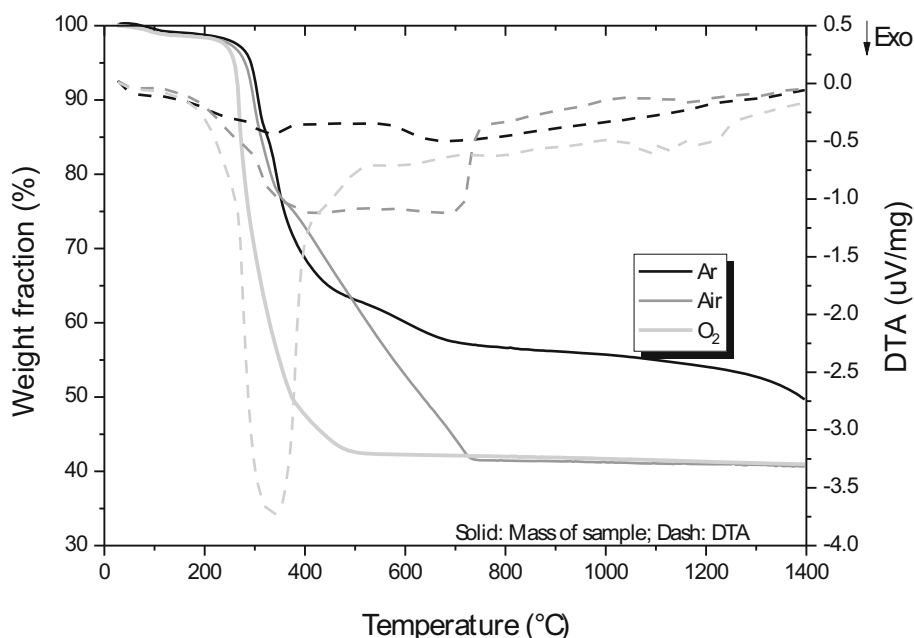


Table 4 Degradation stages of PCBs in Ar, air, and oxygen according to TG analysis

Sample	Stage I		Stage II		Stage III	
	<i>T</i> (°C)	Rate (g/s)	<i>T</i> (°C)	Rate (g/s)	<i>T</i> (°C)	Rate (g/s)
Argon	285–405	2.3266	440–600	0.3124	600–1200	0.0671
Air	275–350	2.4818	375–729	0.9393	749–1394	0.0129
Oxygen	271–364	3.5987	374–495	0.6051	515–1394	0.0167

Table 5 Kinetic parameters of PCBs in argon, air, and oxygen

	Stage I			Stage II		
	<i>E</i> (KJ/mol)	<i>n</i>	<i>A</i> (S ⁻¹)	<i>E</i> (KJ/mol)	<i>n</i>	<i>A</i> (S ⁻¹)
Ar	61.59	1.01	790.67	2.2E-4	0.062	7.4E-4
Air	137.53	1.412	1.8E10	0.112	0.107	5.3E-4
Oxygen	2.5E-4	0.718	0.003	3.7E-4	0.345	0.002

$$k = -Ae^{\frac{-E}{RT}}, \quad (12)$$

where *A* is the pre-exponential factor, also called collision factor (1/min); *E* is the activation energy (J/mole); *R* is the universal gas constant (8.314 J/mole K) and *T* is the absolute temperature. The activation energy is required for the reactants to become products, whereas the pre-exponential in Eq. (12) defines the number of particles actively participating in the reaction per second.

There are two different approaches for the calculation of reaction kinetics of a chemical processes:

- (I) Model-based analysis, which is a mathematical method based on the assumption about the kinetic model of the process. This procedure uses powerful mathematic tools, such as linear and nonlinear regression, where single step and multiple analysis, respectively, are executed to solve a system of differential equations and to obtain a statistical comparison of used models.
- (II) Model free analysis, which is a simple and widely used approach. Using this approach, only the activation energy of the process can be calculated [33].

The data extracted from thermogravimetric analysis can be used to determine the kinetic parameters of the reactions such as activation energy, order of reaction and the pre-exponential factor. It worth noting that Arrhenius' kinetic theory can only be applied to well define individual chemical reactions. At this point, it has said that pyrolysis of PCBs proceeds through a number of simultaneous reactions, which cannot be well defined. Therefore, Arrhenius' equations is used here only as a kind of trend functions and kinetic parameters found cannot be related to a particular chemical reaction. Therefore, these parameters will be called “apparent activation energy,” “apparent rate

constant,” and “apparent pre-exponential factor.” In addition, since pyrolysis and combustion of PCBs generally include complex degradation processes, it is extremely difficult to conduct a full kinetic analysis of such complex systems, using basic kinetic equations. Therefore, Netzsch Thermokinetics software is used to measure these parameters. The software uses both model-based and model free analysis techniques to calculate the kinetic parameters of the reactions. For the calculations, the multiple-linear regression model with a basic reaction model (first order of reaction, s: A–1 → B) is used on the first two stages of degradation where most of the degradation occurs. Table 5 shows the measured apparent activation energy, apparent order of reaction and the apparent pre-exponential factor in the first two degradation stages of all the processes. From these data, the kinetic behavior of the degradation of materials in different stages is observed.

In general, the energy required to break a bond is also called bond dissociation energy. The energy of a molecule is always lower than the energy of individual constituent atoms. During pyrolysis, some energy is supplied to the weak organic compounds to overcome the dissociation energy and break their bonds. Afterwards, new and stronger bonds are formed to create new molecules like CO, CO₂, H₂, H₂O, etc. Since breaking down the molecules requires a much lower amount of energy than the energy produced forming the new ones, that energy is released in the process and is calculated using the DTA curves. In addition, from the TGA curves, the apparent activation energy can be estimated, which—for this particular case—represents the minimum energy required for the degradation of the sample at each stage of analysis.

It is understood from Eqs. (11) and (12) that the higher the activation energy, the slower the reaction. However, if the collision factor is larger, the rate of the reaction

increases. During the first pyrolysis stage of PCBs, the activation energy and reaction order are high due to the complex degradation process of organic molecules, but the collision factor is also high which increases the speed of the degradation process. In the second stage, the apparent activation energy is lower along with the order of the reaction, but the collision factor is also low leading to a slower reaction than at the first stage.

The first degradation stage along the combustion of PCBs with air is fast, but the apparent activation energy during that process is very high (see Table 5). The apparent pre-exponential factor, which gives the information about the number of collisions happening in the course of the reaction, is also very high. This suggests that although the apparent activation energy for the reaction to occur is high, due to the high reaction temperature (approx. 275–364 °C) and the very high collision factor, the intense decomposition of PCBs is possible. In case of combusting PCBs with oxygen, the apparent activation energy is very low, which means that under the given conditions of temperature, the reaction between PCBs and oxygen has a very low kinetic barrier and a strong exothermic reaction. In this particular case, reactions happen almost spontaneously.

The works published by Quan et al. [34] in 2013 and Zhan Zhi-hua et al. [35] in 2011 indicate a similar study regarding kinetic analysis of pyrolysis in nitrogen and combustion in air of PCBs. They determined the Arrhenius pre-exponential factor A and the activation energy using a first order reaction model. According to their results, the activation energy calculated for pyrolysis was $149.28 \text{ kJ mol}^{-1}$ [34] and 212 kJ/mol [35]. Kantaralis has also performed different kinetic pyrolysis tests finding the activation energy at around 88.38 and 95.54 kJ/mol by two iso-conventional methods [21]. As it was mentioned, kinetic calculations cannot be accurately applied to pyrolysis of PCBs. Therefore, these values are only intended to provide hints on the kinetics between the different stages of pyrolysis and combustion (air and oxygen), and compare both processes under same experimental conditions.

Fast Pyrolysis of Shredded PCBs

So far, the degradation mechanisms of organics in PCBs and the off-gas evolution are examined by conducting pyrolysis experiments under low heating rates, which means that the material is fed into the cold reactor and heated up slowly to the final temperature. As a further step, pyrolysis experiments are conducted by applying high heating rates to shredded printed circuit boards. Since the furnace within the experimental setup has got a limited heating rate, the material is charged into the hot reactor, which is heated up to different constant temperatures previously. The off-gas composition during the pyrolysis as

well as the carbon content of the solid residue are measured in order to assess the fast pyrolysis of PCBs.

Off-Gas Analysis

Especially during the experiments at temperatures higher than 500 °C, it becomes apparent that the FTIR reaches its limit concerning the maximum measurement range. Although the pyrolysis gas is diluted with 4 L/min of argon, the overall off-gas concentration is too high to provide proper measuring values in case of some gases, such as phenol. However, further dilution would effect that lower concentrated components will drop below the detection limit. On the whole, the analysis of pyrolysis gases via continuous FTIR is a compromise regarding upper and lower detection limits of different gases. Nevertheless, proper results are obtained for relevant gases like CO_2 , CO , CH_4 , and H_2 .

The measurements obtained from the FTIR show that significant evolution of pyrolysis gas takes place above 400 °C. Figure 7 depicts the concentrations of CO_2 , CO , CH_4 , and H_2 during the fast pyrolysis experiments. At 300 °C, only small amounts of the single gas components are detected up to 100 ppm, so that these results do not appear in Fig. 7. For an appropriate comparison, the scale of the axes is the same in every diagram, although the concentration of CH_4 exceeds the ordinate's limit with a maximum concentration of 134,194 ppm at 700 °C. In case of 400 and 500 °C, the content of H_2 declines very slowly and reaches 0 ppm after 12 and 18 min. Concerning the other gases, the evolution is finished after 8 min at the latest. As the temperature inside the reactor is increased to 600 and 700 °C, the signals become more succinct coming along with higher concentrations and a decreasing off-gas evolution time due to a higher reaction rate. With respect to the curves of CH_4 and H_2 , the effect of intensified bond breaking of long hydrocarbon molecules becomes obvious at 700 °C, which was predicted earlier.

In contrast to the slow pyrolysis, the present measurements show high evolutions of CO_2 and CO at elevated temperatures. Since both CO_2 and CO increase with the temperature, the assumption of oxidation by hydroxyl radicals is confirmed because radical formation is promoted at high temperatures. In order to better examine the temperature dependence of CO_2 and CO , Fig. 8 illustrates the average ratio of the CO_2 and CO concentration. With respect to Fig. 7, an average ratio of 2.84 at 500 °C is not expected, because the two graphs seem to be very similar. Although it has to be considered that the decline of CO is slightly faster than in case of CO_2 , so that the difference of concentrations after the peak is much higher. Generally, the average ratio of CO_2 and CO is shifted from 2.99 at 300 °C below 1 at 600 °C.

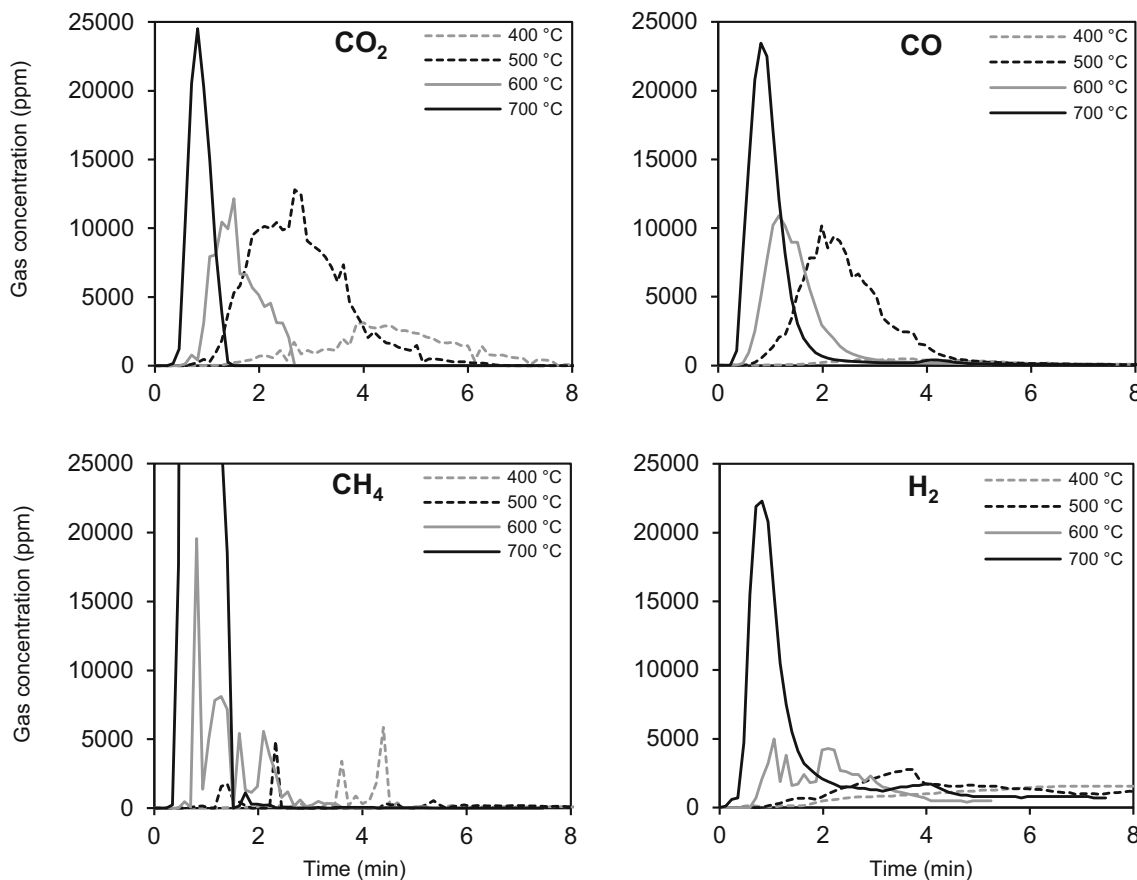
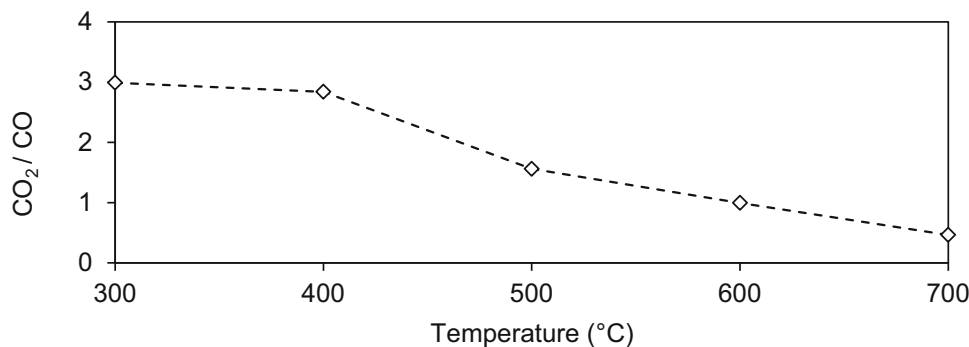
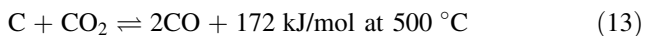


Fig. 7 Concentration of CO₂, CO, CH₄, and H₂ at different pyrolysis temperatures

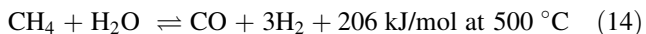
Fig. 8 Average ratio of CO₂ and CO concentration



The increasing amount of CO in relation to CO₂ is effected by the Boudouard reaction and the gasification of char, which is exemplified in the following equation:



With increasing temperatures, the equilibrium is shifted to the right side, causing greater amounts of CO. Another reaction model which has to be taken into account is the so-called reverse methanation reaction [16]:



During this reaction, CH₄, originating from the chain cracking of long hydrocarbons, reacts with steam forming CO and H₂. This model competes with the formation of hydrogen via radical formation, which was explained earlier. However, having a look at Fig. 9, the temperature-dependent concentration of ethane and butane does not disagree with the radical model, since the rapid decline of butane at 700 °C comes along with an increase of ethane and especially CH₄, being products of the cracking of longer molecules, such as butane.

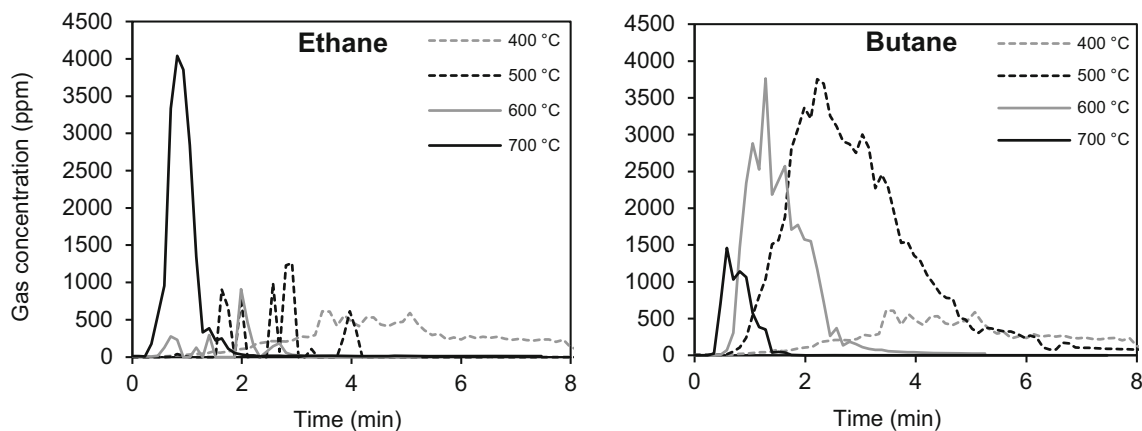


Fig. 9 Concentration of ethane and butane at different pyrolysis temperatures

For HBr, proper results could only be obtained at 700 °C up to 179 ppm. Observations in the works of Barontini and Cozzani as well as Chien et al. correspond with the fact that HBr formation is preferred at high temperatures. However, no HBr is detected below 700 °C, which can be explained by the low concentration of HBr at these temperatures compared to the high concentration of other compounds, which leads to an overlay of the HBr signal in the FTIR.

Carbon Analysis

None of the samples showed a significant peak for total inorganic carbon (TIC), whereas the values for TOC, EC, and TC depend on the pyrolysis temperature, as shown in Fig. 10. Furthermore, the different stages of pyrolysis, as described by Scheirs and Kaminsky, are visible. Up to 600 °C, the decline of TC is strongly connected with the decreasing TOC. Hence, pyrolysis is incomplete and tar, which still contains organic compounds, is formed. From 600 to 700 °C, the amount of TC remains constant, but the concentration of EC exceeds the value of TOC. This fact is

related to the strong dehydrogenation of organics and the preferred formation of char compared to tar.

Comparative Assessment of Slow and Fast Pyrolysis of PCBs

In general, pyrolysis stands among others pre-processing methods to remove or reduce the amount of organic matter presented in WEEE, which enables both an enrichment of the metallic fraction and separation of halides and hazardous materials. In addition, the reduced organic carbon and increased concentration of elemental carbon improves the quality of energy content, which makes the subsequent pyrometallurgical smelting easier to control. All these benefits can only be considered if degradation of organics in electronic scrap during pyrolysis is fairly understood, despite the complex reactions mechanisms occurring during the process, and pyrolysis parameters are optimized to produce better quality products. This work attempts to better understand the degradations mechanisms during pyrolysis and to understand the effect of a fast heating rate in the process.

Fig. 10 Content of organic carbon (TOC), elemental carbon (EC), and total carbon (TC) in the solid residue

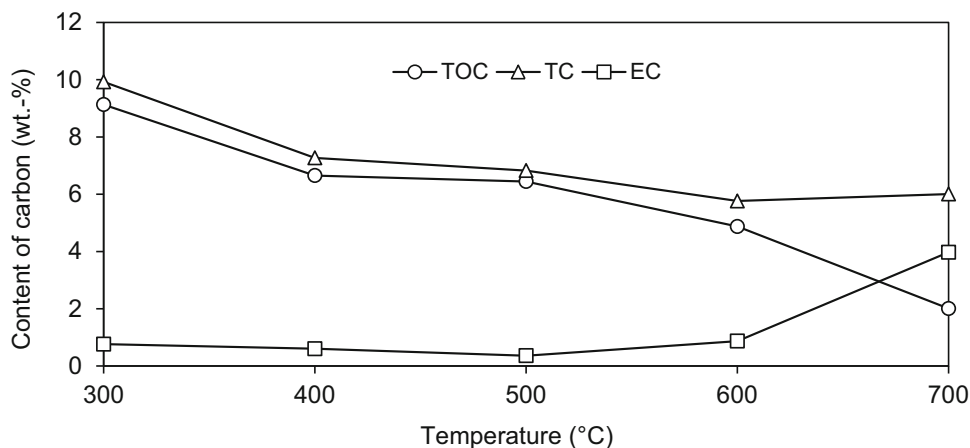


Table 6 depicts an overview of the amounts of evaporated gases during the slow pyrolysis up to 700 °C, as well as the fast pyrolysis at 300, 400, and 700 °C. The amounts are calculated by integrating the time-concentration-records from the FTIR, obtaining total volumes in mL/g referred to the initial dry mass of PCBs. Taking the volumes of H₂O and CO into account, it becomes evident that the reverse methanation reaction, as it is observed in the fast pyrolysis experiments, only plays a subordinated role in pyrolysis processes with slow heating rates, since the major share of water is evaporated prior to the evolution of methane. At high heating rates, the volume of water reaches its maximum of 38.96 mL/g-PCBs at 400 °C and decreases down to 8.83 mL/g at 700 °C. Simultaneously, the amounts of CO and H₂ increase, which indicates the existence of the reverse methanation reaction at 700 °C.

However, the overall volume of hydrogen evolved at slow pyrolysis is even slightly higher than during fast pyrolysis at 700 °C. Therefore, the mechanism of hydrogen generation by formation and recombination of radicals has to be taken into account as well and seems to happen at slow pyrolysis, while tar is thermally decomposed reaching high temperatures. In addition, a considerable difference between fast and slow pyrolysis appears in the volumes of organic compounds, possessing hydroxyl groups (cresol) and aldehyde groups (acetaldehyde, acrolein). Since the amounts of these gases are higher at slow pyrolysis, it can be concluded that both high heating rates and high temperatures effect the separation of oxygen and hydroxyl groups, having the potential to oxidize other components. Comparing the column for fast pyrolysis at 400 °C with the other data, it can be deduced that fast pyrolysis at 400 °C

Table 6 Comparison of the total amount of gases per gram PCB produced between slow and fast pyrolysis

Component	Vol. in mL/g			
	Slow pyrolysis 700 °C	Fast pyrolysis		
		300 °C	400 °C	700 °C
H ₂ O	59.31	10.75	38.96	8.83
H ₂	32.20	1.59	21.84	30.75
H _x C _y	26.90	3.47	15.72	42.99
HCl	13.99	0.25	0.04	0.09
CO	4.01	0.19	1.23	10.75
CH ₄	5.47	0.08	1.69	35.90
CO ₂	5.69	1.69	5.30	7.51
Styrene (C ₈ H ₈)	2.65	0.00	0.61	1.38
Cresol-o (C ₇ H ₈ O)	1.79	0.00	0.00	0.00
Cresol-p (C ₇ H ₈ O)	1.79	0.17	0.33	0.32
Acrolein (C ₃ H ₄ O)	1.93	0.00	0.23	0.01
Acetic acid (CH ₃ COOH)	1.44	0.00	0.00	0.00
Benzene (C ₆ H ₆)	0.91	0.00	0.69	1.43
Acetaldehyde (C ₂ H ₄ O)	0.46	0.01	0.63	0.01
Ethane (C ₂ H ₆)	0.54	0.62	0.14	1.37
Cresol-m (C ₇ H ₈ O)	0.47	0.04	0.33	0.16
Ethylene (C ₂ H ₄)	0.41	0.00	1.91	25.01
HBr	0.09	0.00	0.00	0.22
Phenol (C ₆ H ₆ O)	0.17*	1.25	3.46	1.50
Propene (C ₃ H ₆)	0.16	0.00	0.58	3.07
Propane (C ₃ H ₈)	0.13	0.00	0.00	0.00
Formaldehyde (CH ₂ O)	0.08	0.22	0.51	0.05
Acetone (C ₃ H ₆ O)	0.15	0.03	1.05	0.55
Ethylbenzene (C ₈ H ₁₀)	0.07	0.31	0.90	0.86
Toluene (C ₇ H ₈)	0.00	0.26	0.87	1.37
Hexadecane (C ₁₆ H ₃₄)	0.00	0.00	0.12	0.01
Butane (C ₄ H ₁₀)	0.00	0.47	1.67	0.49
O ₂	0.00	0.00	0.00	0.00

*Values of measured spectrum are below reliable levels

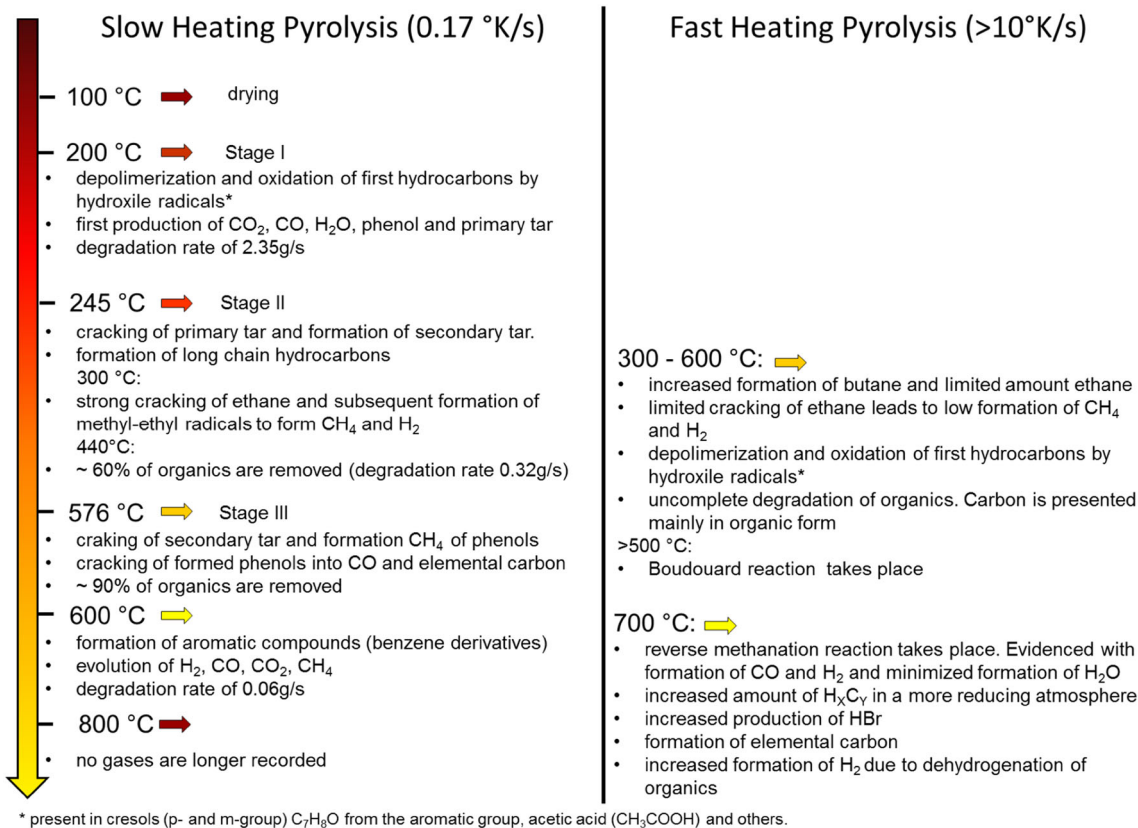


Fig. 11 Main differences between slow heating and fast heating pyrolysis. (Color figure online)

provides the best conditions to form phenol, whereas other aromates, such as toluene and styrene, are rather formed at 700 °C.

Conclusion

According to the pyrolysis gas composition and kinetic analysis, the slow pyrolysis involves at least three stages of organic degradation beside an early dehydration process (< 200 °C). These stages are stage I (220–345 °C), stage II (345–575 °C), and stage III (> 600 °C). From this, 98% of the organics are released from the sample during stage I and stage II. Kinetic analysis also indicated that stage I has a degradation speed approx. 7.5 times faster than stage II.

In Fig. 11, the main findings about degradation mechanisms based on the off-gas composition and TG analysis are presented for the slow as well as fast pyrolysis. From all reactions involved during pyrolysis, at least four mechanisms could be clearly identified according to the main products in the off-gas:

- Since no oxygen production could be identified, it can be concluded that combustion reactions are driven by the presence of free hydroxyl radicals which can be

produced from degradations of C–H–O compounds like cresols, aromatics, and acetic acid.

- The production of CH₄, H₂, and CH₂ is strongly influenced by the degradation from ethane. Ethane breaks its covalent bond above 300 °C forming two methyl molecules. The methyl radicals strip hydrogen radicals from other ethyl molecule to form CH₄ and hydrogen (see Eqs. 6–10). This degradation mechanisms are highly affected by the heating speed and the pyrolysis temperature. According to the results, at lower temperatures (< 600 °C) and fast heating speed, formation of butane is more likely, which decreases drastically due to the formation of CH₄ and hydrogen gas. On the other hand, fast pyrolysis at higher temperature than 600 °C results in an increased formation of ethane, whose degradation leads to a strong formation of CH₄.
- Fast pyrolysis above 600 °C leads to the so called reverse methanation reaction (Eq. 11), which promotes the formation of CO and hydrogen, as well as drastically decreases the production of H₂O. Ultimately, these phenomena provide a more reducing atmosphere, and therefore, a higher heat value of the pyrolysis gas compared to the slow pyrolysis.

– Phenol formation is only clearly evidenced at fast heating pyrolysis with temperatures lower than 500 °C. Most possible mechanism for phenol formation is due to degradation of toluene and benzene by (–OH) hydroxyl radicals, which represents a source of water through hydrogen extraction from any available methylene linkage (supported by [36–39]). However, due to the lack of these radicals, in the fast pyrolysis, increased formation of these gases can be appreciated. It is also known that degradation of benzene at lower temperatures by the –H/OH substitution is more likely to occur compared to the *H abstraction from the aromatic ring [37, 38, 40]. This explains why phenol formation at lower temperatures than 500 °C is more favorable. Toluene, on the other hand, could also derivate to methylphenols like cresols by partial oxidation reactions [41], which could not be completely oxidized as no free oxygen in the system was detected as well as limited amount of other C–H oxidants. From the results, degradation of toluene could be expected at 400 °C since formation of cresols obeys similar trends to the toluene detection in the fast pyrolysis.

Carbon is present in electronic scrap as organic material originating mainly from epoxy resins and thermoplastics. Above 600 °C, carbon in the sample remains almost identical in concentration but in the form of very fine elemental carbon. From the process point of view, this reduces not only generation of off-gas in the pyrometallurgical smelting, but also improves the reduction efficiency of copper oxide from the slag by the generation of CO bubbles (foam slag) in the combustion process rather than producing direct combustion of the organic gases in the gas phase.

Acknowledgement This study is supported by the cooperation project RessourcenKollég.NRW, funded by the North Rhine-Westphalia Ministry of Science. Special thanks to Prof. Flamme for the constructive discussion and for providing the test material used for this study.

References

- Balde CP (2015) The global e-waste monitor 2014: quantities, flows and resources. United Nations University, Bonn
- Robinson BH (2009) E-waste: an assessment of global production and environmental impacts. *Sci Total Environ* 408:183–191
- Namias J (2013) The future of electronic waste recycling in the United States: obstacles and domestic solutions. Master Thesis, Columbia University
- Luyima A (2013) Recycling of electronic waste: printed wiring boards: printed wiring boards. Doctoral Dissertations
- Kim B-S, Lee J-C, Seo S-P, Park Y-K, Sohn HY (2004) A process for extracting precious metals from spent printed circuit boards and automobile catalysis. *JOM* 56:55–58
- Yokoyama S, Iji M (1997) Recycling of printed wiring boards with mounted electronic parts. *Circuit World* 23:109–114
- Zhao Y, Wen X, Li B, Tao D (2004) Recovery of copper from printed circuit boards. *Miner Metal Process* 21:99–102
- Luda MP (2012) Waste electrical and electronic equipment (WEEE) handbook: pyrolysis of WEEE plastics. Woodhead Publishing, Cambridge
- Damoah L, Zuo X, Zhang L, Schuman T, Kers J (2011) Green pyrolysis of used printed wiring boards powders. In: Lifeng Z, Krundick GK (eds) *Recycling of electronic waste II: proceedings of the second symposium*. Wiley, Hoboken
- Eppe B, Leithner R, Linzer W, Walter H (2009) *Simulation von Kraftwerken und wärmetechnischen Anlagen*, New York
- Thomé-Kozmiensky KJ, Pahl U (eds) (1994) *Thermische Abfallbehandlung, 2., völlig neu bearb. Aufl. ed., EF-Verl. für Energie- und Umwelttechnik*, Berlin
- Thomé-Kozmiensky KJ (ed) (1985) *Pyrolyse von Abfällen, 1. Aufl. ed., EF-Verl. für Energie- und Umwelttechnik*, Berlin
- Cui J, Zhang L (2008) Metallurgical recovery of metals from electronic waste: a review. *J Hazard Mater* 158:228–256
- Mankhand TR, Singh KK, Gupta SK, Das S (2012) Pyrolysis of printed circuit boards. *Int J Metall Eng* 1:102–107
- Moss GP, Smith PAS, Tavernier D (1995) Glossary of class names of organic compounds and reactivity intermediates based on structure (IUPAC Recommendations 1995). *Pure Appl Chem* 67:1307–1375
- Basu P (2010) *Biomass gasification and pyrolysis: practical design and theory*. Elsevier, Amsterdam
- Devi L, Ptasiński KJ, Janssen FJJG (2003) A review of the primary measurement for tar elimination in biomass gasification process. *Biomass Bioenerg* 24:125–140
- Neef JPA, Knoef HAM, Zielke U (1999) Guideline for sampling an analysis of tar and particles in biomass producer gas 3.1, Energy project
- Milne TA, Evans RJ (1998) Biomass gasifier tars: their nature, formation, and conversion, National Renewable Energy Laboratory
- Evans RJ, Milne TA (1997) Chemistry of tar formation and maturation in the thermochemical conversion of biomass. *Developments in Thermochemical Biomass Conversion*. Springer, Netherlands
- Kantarelis E (2009) Thermochemical treatment of electric and electronic waste thermochemical treatment of electric and electronic waste for energy recovery. Licentiate Thesis, Stockholm
- Mayers MA (1934) The combustion of carbon. *Chem Rev* 14:31–53
- Diaz F, Florez S, Friedrich B (2015) Mass flow analysis and metal losses by the degradation process of organic-containing WEEE scraps. *Chem Ing Tech* 87:1599–1608
- Luda MP (2011) Integrated waste management—volume II: recycling of printed circuit boards. InTech, Lurago Marinone, Italy
- Jie G, Ying-Shun L, Mai-Xi L (2008) Product characterization of waste printed circuit board by pyrolysis. *J Anal Appl Pyrol* 83:185–189
- Barontini F, Cozzani V (2006) Formation of hydrogen bromide and organobrominated compounds in the thermal degradation of electronic boards. *J Anal Appl Pyrol* 77:41–55
- Chien YC, Wang HP, Lin KS, Huang Y-J, Yang YW (2000) Fate of bromine in pyrolysis of printed circuit board wastes. *Chemosphere* 40:383–387
- Scheirs J, Kaminsky W (eds) (2006) *Feedstock recycling and pyrolysis of waste plastics: converting waste plastics into diesel and other fuels*. Wiley, Chichester, Hoboken
- Mishra DP (2014) *Experimental combustion*. CRC Press, Boca Raton

30. Lin MC, Back MH (1966) The thermal decomposition of ethane: Part I. Initiation and termination steps. *Can J Chem* 44:505–514
31. Lin MC, Back MH (1966) The thermal decomposition of ethane: Part II. The unimolecular decomposition of the ethane molecule and the ethyl radical. *Can J Chem* 44:2357–2367
32. Wendlandt W (1974) *Thermal Methods of Analysis*, 2nd edn. Wiley, New York
33. NETZSCH (2016) Thermokinetics. <https://www.netzsch-thermal-analysis.com/en/products-solutions/software/netzsch-advanced-software/thermokinetics/#!#c278832>. Accessed 19 Sep 2016
34. Quan C, Li A, Gao N (2013) Combustion and pyrolysis of electronic waste: thermogravimetric analysis and kinetic model. *Proced Environ Sci* 18:776–782
35. Zhan Z-H, Qiu K-Q (2011) Pyrolysis kinetics and TG-FTIR analysis of waste epoxy printed circuit boards. *J Cent South Univ Technol* 18:331–336
36. Zhang H-Y, McKINNON JT (1995) Elementary reaction modeling of high-temperature benzene combustion. *Combust Sci Technol* 107:261–300
37. Seta T, Nakajima M, Miyoshi A (2006) High-temperature reactions of OH radicals with benzene and toluene. *J Phys Chem A* 110:5081–5090
38. Suh I, Zhang D, Zhang R, Molina LT, Molina MJ (2002) Theoretical study of OH addition reaction to toluene. *Chem Phys Lett* 364:454–462
39. Jackson WM, Conley RT (1964) High temperature oxidative degradation of phenol–formaldehyde polycondensates. *J Appl Polym Sci* 8:2163–2193
40. Hollman DS, Simmonett AC, Schaefer HF (2011) The benzene+ OH potential energy surface: intermediates and transition states. *Phys Chem Chem Phys* 13:2214–2221
41. Kaeding WW, Lindblom RO, Temple RG, Mahon HI (1965) Oxidation of toluene and other alkylated aromatic hydrocarbons to benzoic acids and phenols. *Ind Eng Chem Proc Des Dev* 4:97–101